Sundaria, Ravi; Daem, Andries; Osemwinyen, Osaruyi; Lehikoinen, Antti; Sergeant, Peter; Arkkio, Antero; Belahcen, Anouar

Effects of stator core welding on an induction machine – Measurements and modeling

Published in:
Journal of Magnetism and Magnetic Materials

DOI:
10.1016/j.jmmm.2019.166280

Published: 01/04/2020

Document Version
Peer reviewed version

Please cite the original version:
Sundaria, R., Daem, A., Osemwinyen, O., Lehikoinen, A., Sergeant, P., Arkkio, A., & Belahcen, A. (2020). Effects of stator core welding on an induction machine – Measurements and modeling. *Journal of Magnetism and Magnetic Materials*, *499*, [166280]. https://doi.org/10.1016/j.jmmm.2019.166280

Effects of Stator Core Welding on an Induction Machine - Measurements and Modeling

Ravi Sundaria[a,*], Andries Daem[b,*], Osaruyi Osemwinyen[a], Antti Lehikoinen[c], Peter Sergeant[b], Antero Arkkio[a], Anouar Belahcen[a,d]

[a]*Department of Electrical Engineering and Automation, Aalto University, Espoo, Finland*
[b]*Department of Electrical Energy, Metals, Mechanical Constructions and Systems, Ghent University, Ghent, Belgium*
[c]*Smeklab Limited, Espoo, Finland*
[d]*Department of Electrical Power Engineering and Mechatronics, Tallinn University of Technology, Tallinn, Estonia*

Abstract

There is a growing interest towards increasing the efficiency of electrical machines to reduce the ecological footprint. The efficiency of an electrical machine is closely related to the understanding and accurate estimation of the associated losses. One loss component is related to the welding of the electrical steel sheets as a part of manufacturing. This paper studies the effect of the core welding on a typical industrial induction motor. The effect of core welding on the magnetic permeability and core losses is first analyzed with the help of magnetic measurements on the unwelded and welded ring cores assembled from the stator sheets. Further, the derived material parameters are applied in finite element analysis of the induction machine and the effect of welding on the machine performance parameters is analyzed. It was observed that stator core losses increased about 10% due to the welding effect. A mock-up prototype is then manufactured to measure the stator core losses which follow the simulated values closely.

Keywords: `Core loss, Electrical Machines, Steel Sheets, Welding`

1. Introduction

Worldwide, the CO2 emission standards are getting more stringent, which is encouraging to build more efficient and sustainable electrical machines. To achieve the goal of reaching a higher efficiency, one course of action is to improve the production process of electrical machines by studying the impact of each step [1, 2]. A frequently applied technique in this process is welding of the stator laminations, which is known to severely decrease the machine efficiency. This problem should be tackled using a combined effort and interdisciplinary approach of metallurgists, material scientists, and electrical engineers.

Two welding techniques often used are tungsten inert gas (TIG) welding and laser welding. Reference [3] compared the joint strength and additional iron losses for both techniques and found that laser welding, although less strong, yields the least additional iron losses. Also, the properties of the welding joint are determined by several process parameters.

The iron losses occurring in the welded stator laminations have been studied and reported [4, 5, 6, 7, 8, 9]. Most authors agree regarding the various parasitic effects of welding on the iron losses. The welding heat introduces residual stresses in the steel which deteriorate the magnetic properties [3, 4]. The welding seam forms an electrically connected volume on the outer edge of the lamination where local eddy currents can occur [3, 6]. These local eddy current losses rise with an increasing weld seam radius. Lastly, the welding seam can, in combination with stochastically occurring interlaminar contacts due to edge burr or locally weak insulation coating, form eddy current circuits which can create local overheating and damage the core [5, 10].

Modeling of welding effects with finite element (FE) analysis of electrical machine is still a challenge due to the complex nature of the associated physical phenomenon. The welding effect can be classified in broadly two phenomena. One deals with the local eddy currents in the iron bars resulting from the welding process. Secondly, there will be magnetic material degrada-

*Ravi Sundaria and Andries Daem contributed equally.
Email addresses: ravi.sundaria@aalto.fi (Ravi Sundaria), andries.daem@ugent.be (Andries Daem)

tion near the welding area due to the generated thermal stresses. Reference [5] studied the interlaminar eddy currents with the help of 3-D FE analysis while [6] proposed an analytical method to model the eddy currents in the welded region. The effect of thermal stresses and changes of microstructure are neglected in [5, 6]. Further, [7] proposed the application of circuit equation coupled FE analysis to model the eddy currents in interlocking dowels. The effect of welding on the core losses, drawn current and efficiency is included in terms of building factors for fractional kilowatt motors in [11]. The effect of welding on low power permanent magnet machines with air winding was studied in [4]. Further, most of the studies are restricted to the study of welded steel laminations [1, 3, 9] and the welding effect on the electrical machine performance is not researched extensively.

This paper studies the effect of welding in a typical industrial induction motor (37 kW induction motor). An engineering approach is adopted to analyze the effect of welding in the FE analysis of the induction motor. The method section describes the procedure to obtain the magnetic measurement from a stack of unwelded and welded ring cores assembled from the stator laminations. Subsequently, a FE model of the motor and a dummy blocked rotor test set up termed as "mock-up test setup" for measurement of stator core losses are also presented. The results section comprises of simulated and measured results on the studied ring cores and induction motor. Finally, a brief discussion with concluding remarks is summarised in the last two sections. It is worth noting that in this paper the shrink-fitting stresses as presented in [12, 13] are not studied, as the purpose is to quantify the effect of welding first.

2. Method

This section is divided into three subsections; first, the ring core measurement test setup is described. The second subsection includes details of the FE model of the studied induction motor. The last subsection describes the mock-up test for measurement of the stator core losses.

2.1. Magnetic measurements on ring cores

Magnetic measurements are performed on the ring cores assembled from the stator sheets of the studied 37 kW induction motor. Nonoriented electrical sheets of grade M400-50A are investigated. Two sets of ring cores are considered; one with the stacked loose sheets termed as "unwelded" while another one is welded with

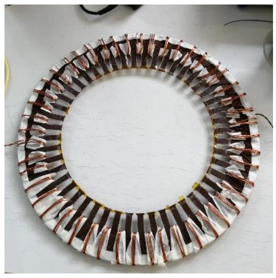

Figure 1: Ring core assembled from the stator laminations.

laser welding and termed as "welded" in this paper. The welded stack consists of 10 sheets with 13 welding points equally distributed along the outer surface. The ring core is magnetized in circumferential direction. The laser welding is performed by Trumpf Trulaser Cell 3000. The automated process of the solid state fiber laser welding should ensure the reliable reproducibility of the welding points. The ring core is presented in Fig. 1. The studied ring cores are wounded with primary and secondary winding each having 144 turns. The secondary voltage is controlled to generate sinusoidal flux in the samples and peak values of magnetic flux density (B) in Tesla (T) and magnetic field strength (H) in Ampere/Meter (A/m) are recorded. Moreover, four different sinusoidal frequencies are considered; 20 Hz, 50 Hz, 100 Hz and 200 Hz. The respective power losses are calculated from the area of the measured BH loops. The three component core loss formula (1) is applied to segregate the core losses in hysteresis, eddy current and excess losses. The loss coefficients are derived with the help of the least square curve fitting toolbox of MATLAB. Here, P is power loss in W/kg at B (T) and excitation frequency f (Hz). The hysteresis, eddy current and excess loss coefficient are denoted by C_h, C_e and C_{ex} respectively.

$$P = C_h B^2 f + C_e B^2 f^2 + C_{ex} B^{1.5} f^{1.5} \quad (1)$$

2.2. FE simulation of induction motor

A typical industrial cage induction motor is studied to analyze the effect of the welding on the machine performance parameters. The studied 4 pole, 37 kW cage induction motor comprises of 48 stator slots, 40 rotor bars and a distributed winding having two parallel paths with 12 conductors in each slot. The time stepping 2-D FE analysis is performed based on the voltage source model. FE analysis is based on the well known magnetic vector potential based AV formulation. One pole of the motor is simulated and the mesh consists of 1516

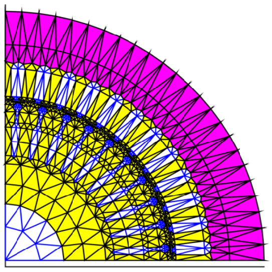

Figure 2: One pole of the induction motor with different material applied for the stator yoke and other iron parts represented by magenta and yellow colors respectively.

second order elements with 3085 nodes. The effects of stator end windings and rotor bars are modeled with the respective impedances in the circuit equations.

The core welding will cause local eddy currents, thermal and mechanical stresses. Individual modeling of these complex physical phenomena is not in the scope of the paper. Rather these phenomena are lump together as a *global* degradation. This is done by assigning a different material to the stator yoke than the rest of the motor iron as presented in Fig. 2. The yoke material parameters in the welded case are derived from the magnetic measurements of the welded ring core stack which have same number of welding points. The yoke material of the studied 37 kW cage induction motor is considered uniformly degraded as a result of the welding to simulate the welding effect on the motor performance. The simulations were carried for both unwelded and welded cases. The motor core losses and supply current are calculated as result of the FE simulation in contrast of the building factor approach of [11].

2.3. Mock-up test setup

Based on the presented simulation results of the 37 kW cage induction motor in the result section it can be observed that the stator core losses are affected the most due to the welding effect. Therefore, the authors proceeded to manufacture a blocked rotor test setup termed as “mock-up test set up” for the accurate measurement of the stator core losses. The stator geometry and winding configuration of the mock-up test setup are identical to the 37 kW induction motor. However, the rotor does not have any rotor bars or rotor slots. The rotor is built from the same electrical steel as the stator. The parameters of the laser welding and number of the weld spots on the stator of the actual machine are same as the “welded” ring core. The stator and rotor are cut with electric discharge wire (EDM) cutting. EDM cutting is known to produce significantly low stresses and changes in the microstructure of the material compared with punching or laser cutting, hence removing partially the need to consider the cutting related losses in the simulations and measurements [14]. The blocked rotor condition will help in avoiding the inclusion of the friction losses in the total measured losses. The welded stator was not shrink fitted with the frame hence the corresponding losses due to the compressive stresses are also not included in the measurements and simulations. It is worth noting that the measurements presented in this paper are carried out on the mock-up setup. As according to the simulations, the flux density distribution in the stator of the mock-up is similar to the one in the real motor, the real motor has not been measured. The purpose of this procedure is to enable discriminating the effect of welding in both the simulations and the measurements and thus serves the purpose of this study. The mock-up test setup is presented in Fig. 3.

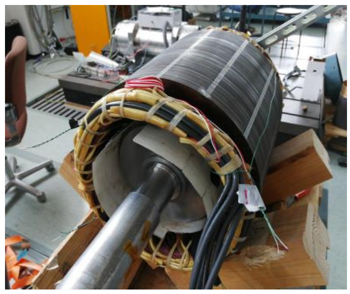

Figure 3: Mock up test setup with dummy blocked rotor.

3. Results

This section is divided into three subsections. First the magnetic measurements on unwelded and welded ring cores are presented. The effect of welding on the 37 kW induction machine is analyzed in the subsequent subsection with the help of FE analysis. The final subsection includes the simulation and measurement results of the mock-up test setup to study the effect of welding on the stator core losses.

3.1. Magnetic measurements on ring cores

Magnetic measurements are performed on the unwelded and welded ring cores described in section 2.1. The obtained single value *BH* curves in the form of a peak of *B* and *H* are presented in Fig. 4. It can be observed that the magnetic permeability has decreased due to the welding effect. Similarly, the specific core loss density at different values of peak magnetic flux density is measured. Fig. 5a and Fig. 5b present the measured

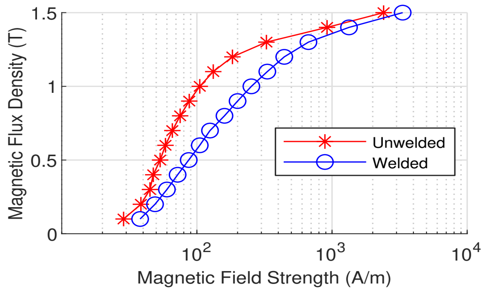

Figure 4: Magnetic measurements of magnetization curve at 50 Hz of unwelded and welded ring core samples.

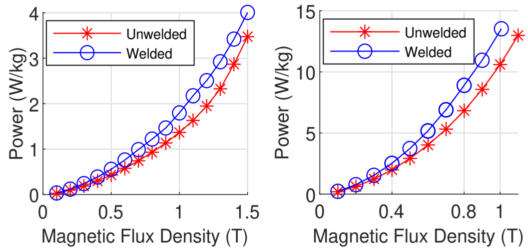

(a) (b)

Figure 5: Core loss measurements of unwelded and welded ring core samples at (a) 50 Hz (b) 200 Hz.

core loss density at 50 Hz and 200 Hz respectively. The effect of welding can be observed in terms of increased core losses in the welded sample as compared to the unwelded sample.

Further, the core loss coefficients (1) are obtained from the least square curve fitting and results are summarized in the Table 1. The excess loss coefficient shows the largest increase due the welding effect.

3.2. *Welding effect on induction motor*

A time stepping FE analysis of the 37 kW cage induction motor is performed at two different load conditions i.e. no load and full load. The effect of welding is considered in the yoke material in terms of *BH* curves and core loss coefficients derived from the welded ring core measurements. The results are summarized in Table 2 and Table 3 for no load and full load conditions. The motor performance parameters such as supply current (I_s), core losses (P_c), torque (T) are analyzed. The no load current has increased about 4 % due to the decreased magnetic permeability of the yoke material as a result of the welding effect. Further, a significant increase in the range of about 10% has been observed in the stator core losses (P_{cs}) at both the studied load conditions. The segregation of the stator core losses in terms

Table 1: Core loss coefficients

	Unwelded	Welded	% Difference
C_h	0.020	0.021	5
C_e	1.5×10^{-4}	1.8×10^{-4}	20
C_{ex}	2.7×10^{-4}	8×10^{-4}	196

Table 2: Welding effect at no load

	Unwelded	Welded	% Diff.
I_s (A)	32	33.4	4
P_c (W)	332	359	8
P_{cs} (W)	256	285	10
P_{hy} (W)	166	167	0.6
P_e (W)	74	79	7
P_{ex} (W)	17	39	108

I_s-supply current, P_c-core losses, P_{cs}-stator core losses, P_{hy}-hysteresis loss, P_e-eddy current loss, P_{ex}-excess loss.

Table 3: Welding effect at full load

	Unwelded	Welded	% Diff.
I_s (A)	67.45	68	0.8
T (Nm)	230.1	230.2	0.04
P_c (W)	390	421	8
P_{cs} (W)	297	328	10
P_{hy} (W)	166	167	0.5
P_e (W)	103	109	6
P_{ex} (W)	28	52	90

of hysteresis (P_{hy}), eddy current (P_e) and excess losses (P_{ex}) is also presented. The effect of welding on the full load current and torque is negligible as compared to the core losses.

3.3. *Core loss simulations and measurements with mock-up setup*

From the simulation results it is clear that mainly, the core losses are affected due to the welding effect as compared to the other parameters such as torque, full load current, etc. Therefore, this section focuses on reliable and accurate measurement of the stator core losses to study the welding effect with the help of "mock-up test set up" described in section 2.3. Fluke Norma 4000 power analyzer recorded the supply voltage, current, frequency and power measurements. The measured total power consists of copper losses and core losses. The core losses are calculated by subtracting the copper losses from the total losses. Finally, the measured stator core losses are obtained removing the simulated

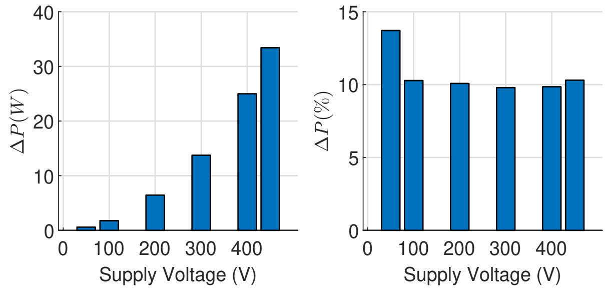

(a) (b)

Figure 6: Increase in simulated stator core losses of mock-up test setup due to the effect of welding at 50 Hz and different supply voltages . (a) absolute values (b) relative values.

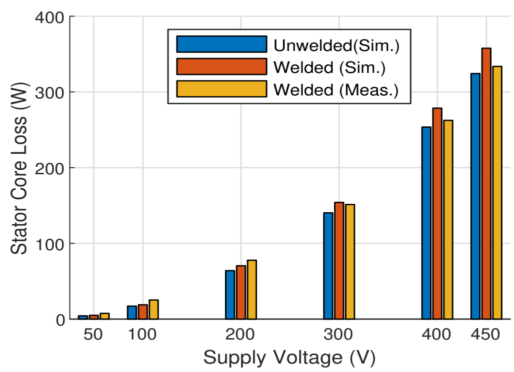

Figure 7: Simulated and measured stator core losses of mock-up test setup at 50 Hz and different supply voltages.

rotor core losses from the measured core losses. There is a clear increase in the simulated stator core losses as a result of the welding effect as presented in terms of absolute and relative values in Fig. 6a and Fig. 6b respectively. The increase is about 10% across the supply voltages. Fig. 7 presents the simulated and measured stator core losses at different supply voltages at 50 Hz i.e. different magnetic flux levels (V/f ratio) in the machines. The measured stator core losses of the mock-up test setup closely follow the simulated values when the welding effect was considered in the FE analysis. The relatively high error in the measured values at 400V and 450V may be the result of the limited range of ring core measurements in deriving the loss coefficients. The ring core measurements are performed upto the magnetic flux density of 1.5 T. However, at 400V (rated) and 450V (over rated), the magnetic flux density was observed in the range of 1.8 T especially in the stator teeth as shown in the Fig. 8.

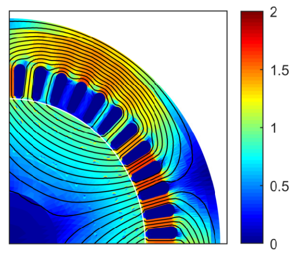

Figure 8: Flux density distribution at 400V and 50 Hz supply.

4. Analysis and Discussion

The studied motor show about 10% increase in the stator core losses due to the welding. If the motor is scaled by changing the axial length keeping other dimension same; the welding effect should be same i.e. about 10%. This is due relatively no change in the respective radial field distribution. Further, similar observation about scale up were reported in [11] for different machines.

Indeed it is difficult to generalize the effect of welding across machines of different power ratings, topologies, core material and welding techniques. For example, reference [11] showed 20% increase in the stator core losses (yoke region) due to welding in the fractional kilowatt motors. The fraction kilowatt motors have lower yoke width as compared to the motor studied in this paper which may result in a higher welding effect. Ideally, to make a generalized welding loss model, measurements and modeling should be performed at local level rather than at a global one as was done in this study.

5. Conclusion

This paper studies the effect of core welding on electrical machines. The core welding is performed as part of the manufacturing of electrical machines. Ring core measurements on unwelded and welded sheets are performed which show a significant effect on the measured permeability and core losses. Further, the simulation results of 37 kW induction motor show that the stator core losses are affected the most due to the welding. A mock-up test setup was proposed and manufactured to measure the stator core losses accurately. Further, a method is presented to include the effect of welding in the FE simulation of the motor by considering the yoke region uniformly degraded. The yoke region magnetic properties are derived from the unwelded and welded ring cores. Both the measurements and simulations result in about 10% increase in the stator core losses in the studied motor. As a significant impact of welding is observed in a typical industrial motor in this research work, it should motivate the research community to investigate this challenging and important research area further.

Acknowledgements

This research work has received funding from the European Research Council under the European Unions Seventh Framework Programme (FP7 /2007-2013) / ERC Grant Agreement n. 339380 and NWO−Vlaio project IWT 150457 high efficiency, high speed electrical drives.

References

[1] T. T. Osamu Nakazaki, Yuichiro Kai, M. Enokizono, Iron loss properties of a practical rotating machine stator core at each manufacturing stage, INT. J. APPL. ELECTROM. 33 (2010) 79 – 86 (2010).

[2] A. Schoppa, J. Schneider, C.-D. Wuppermann, Influence of the manufacturing process on the magnetic properties of non-oriented electrical steels, J. Magn. Magn. Mater. 215-216 (2000) 74 – 78 (2000).

[3] Y. Zhang, H. Wang, K. Chen, S. Li, Comparison of laser and tig welding of laminated electrical steels, J. Mater. Process. Technol. 247 (2017) 55 – 63 (2017).

[4] A. Krings, S. Nategh, O. Wallmark, J. Soulard, Influence of the welding process on the performance of slotless pm motors with sife and nife stator laminations, IEEE Trans. Ind. Appl. 50 (1) (2014) 296–306 (Jan 2014).

[5] P. Handgruber, A. Stermecki, O. Bíró, G. Ofnery, Evaluation of interlaminar eddy currents in induction machines, in: IECON 2013 - 39th Annual Conference of the IEEE Industrial Electronics Society, 2013, pp. 2792–2797 (Nov 2013).

[6] H. Wang, Y. Zhang, Modeling of eddy-current losses of welded laminated electrical steels, IEEE Trans. Ind. Electron. 64 (4) (2017) 2992–3000 (April 2017).

[7] M.-J. J. Gui-Yu Zhou, He Hao, J.-X. Shen, Influence of interlocking dowels on motor core loss, COMPEL 35 (2) (2016) 808–820 (2016).

[8] K. Bourchas, A. Stening, J. Soulard, A. Broddefalk, M. Lindenmo, M. Dahlén, F. Gyllensten, Quantifying effects of cutting and welding on magnetic properties of electrical steels, IEEE Trans. Ind. Appl. 53 (5) (2017) 4269–4278 (Sep. 2017).

[9] A. Schoppa, J. Schneider, C.-D. Wuppermann, T. Bakon, Influence of welding and sticking of laminations on the magnetic properties of non-oriented electrical steels, J. Magn. Magn. Mater. 254-255 (2003) 367 – 369, proceedings of the 15th International Conference on Soft Magnetic Materials (SMM15) (2003).

[10] M. C. Marion-Pera, A. Kedous-Lebouc, T. Waeckerle, B. Cornut, Characterization of SiFe sheet insulation, IEEE Trans. Magn. 31 (4) (1995) 2408–2415 (July 1995).

[11] Z. Gmyrek, A. Cavagnino, Influence of punching, welding, and clamping on magnetic cores of fractional kilowatt motors, IEEE Trans. Ind. Appl. 54 (5) (2018) 4123–4132 (Sep. 2018).

[12] D. Miyagi, N. Maeda, Y. Ozeki, K. Miki, N. Takahashi, Estimation of iron loss in motor core with shrink fitting using fem analysis, IEEE Trans. Magn. 45 (3) (2009) 1704–1707 (March 2009).

[13] N. Takahashi, H. Morimoto, Y. Yunoki, D. Miyagi, Effect of shrink fitting and cutting on iron loss of permanent magnet motor, J. Magn. Magn. Mater. 320 (20) (2008) e925 – e928, proceedings of the 18th International Symposium on Soft Magnetic Materials (2008).

[14] M. Hofmann, H. Naumoski, U. Herr, H. Herzog, Magnetic properties of electrical steel sheets in respect of cutting: Micromagnetic analysis and macromagnetic modeling, IEEE Trans. Magn. 52 (2) (2016) 1–14 (Feb 2016).